Nonlinear Response Analysis of a Chord-Wise Flexible Flapper in the Wake of a Bluff Body using OpenFOAM

Rajanya Chatterjee[1], Chandan Bose[2], Sayan Gupta[1] & Sunetra Sarkar[1]

1. *Indian Institute of Technology Madras, Chennai 600036, India, rajanya02@gmail.com, gupta.sayan@gmail.com, sunetra.sarkar@gmail.com*
2. *University of Liege, Liege 4000, Belgium, cb.ju.1991@gmail.com*

The efficient propulsion of the natural swimmers involves complex Fluid-Structure Interactions (FSI) between their highly deformable body and the wake generated by upstream obstacles, especially during the passive swimming phase. The swimming fishes often synchronize their body deformation profile with the oncoming wake vortices in order to optimize the swimming efficiency by applying a control forcing. Structurally, the fish body is often modeled as a free-free or cantilever beam with a travelling wave along the body, representative of their self-controlled muscle activity [1]. Such a bio-inspired configuration - a flexible flapper situated downstream of a cylinder - has significant potential in flow energy harvesting [2], and can also be used as an active vorticity control mechanism [3]. In these contexts, the flow-induced vibration of a cantilever beam has been studied by several groups [4] to understand the effects of different structural parameters, such as the flapper length, flexibility, mass-ratio among many other design parameters. However, the effects of different upstream bluff-body shapes and the relative position of the flapper on the nonlinear dynamical behavior of this FSI system remain largely unexplored in the literature. There is also a lack of understanding on the implications of different dynamical regimes of this system on the energy harvesting potential and the life of the harvester. A thorough understanding of the underlying vortex interactions will enable us to tune the vortex-shedding frequency in connection with the natural frequency of the flapper to maximize the power output. The present study aims to take up these investigations.

Computational Methodology

The high-fidelity FSI simulations can be based on either monolithic or partitioned approach [5]. In the monolithic approach, both the structural and fluid governing equations are solved in a single mathematical and computational framework with implicit interfacial conditions. On the other hand, two different existing solvers are coupled in the partitioned approach to solve the two separated sub-systems of fluid and solid models. Again, in the partitioned approach, there exist two different coupling strategies [5]: weak and strong coupling. Although the weak coupling could be an affordable choice in terms of the associated computational cost, it can lead to a time-lagged solution and numerical instabilities especially when the fluid and solid

densities are comparable for a very flexible structure with large deformation, leading to unphysical instabilities. On the contrary, the strong coupling strategy demands solving the sub-systems multiple times until the convergence criterion at the interface is satisfied, thus ensuring a better accuracy. In this study, we have adopted a partitioned strong-coupling strategy available in the fsiFOAM [6] solver of OpenFOAM.

Governing Equations

The FSI framework of fsiFOAM [6] is composed of an incompressible Navier-Stokes (N-S) solver, strongly coupled by a partitioned approach with a nonlinear elastic structural model. The viscous flow-field, governed by an incompressible N-S equation, can be cast into arbitrary Lagrangian-Eulerian (ALE) formulation [7] as

$$\nabla . \vec{\boldsymbol{u}} = 0, \tag{1}$$

$$\frac{\partial \vec{\boldsymbol{u}}}{\partial t} + [\vec{\boldsymbol{u}} - \vec{\boldsymbol{u}}^m) . \nabla] \ \vec{\boldsymbol{u}} \ = \ -\nabla p/\rho + \nu \, \nabla^2 \vec{\boldsymbol{u}} \, . \tag{2}$$

Here, $\vec{u}$ is the flow velocity, $\vec{u}^m$ is the grid point velocity, p is the pressure, ρ is the fluid density and ν is the kinematic viscosity. The flexible flapper is modelled as an elastic continuum with its leading-edge restrained as a fixed support. Mathematically, conservation of linear momentum is given by

$$\frac{\partial}{\partial t} \int \rho_s \boldsymbol{v} \, dV \ = \ \oint \boldsymbol{n} . \boldsymbol{\sigma} \, d\Gamma + \int \rho_s \boldsymbol{b} \, dV \ \ , \tag{3}$$

where, V is the volume of the flapper bounded by the surface Γ with unit normal $\boldsymbol{n}$, $\boldsymbol{v}$ is the velocity vector, $\boldsymbol{\sigma}$ is the Cauchy stress tensor, ρ_s is the density of the material of the structure and $\boldsymbol{b}$ is the body force perunit mass. Assuming large strain, the material behaviour of the flapper has been modelled using St. Venant-Kirchhoff hyper-elasticity theory. The linear momentum equation can therefore be written in terms of the second Piola-Kirchhoff stress tensor (S) as $\boldsymbol{\sigma} = \frac{1}{J} \boldsymbol{F} . \boldsymbol{J} . \boldsymbol{F}^T$; $\boldsymbol{F} = \boldsymbol{I} + \boldsymbol{\Delta w}$ is the deformation gradient, $\boldsymbol{I}$ is the identity tensor and w is the deformation vector. According to the constitutive model for the St. Venant-Kirchhoff material, $\boldsymbol{S}$ can be designed as $\boldsymbol{S} = \lambda (tr \, \boldsymbol{E}) I + 2\mu \boldsymbol{E}$, where $\boldsymbol{E} = \frac{1}{2} (\boldsymbol{F}^T \boldsymbol{F} - I)$ and λ and μ are Laḿe constants ('tr' denotes the trace of a matrix).

Numerical Algorithms

The incompressible N-S equation has been discretized on a moving grid with a Laplacian mesh motion strategy [6]. The flow solver uses a second order accurate spatial discretization and the temporal discretization is performed using a second order implicit backward differencing

scheme. A variable time stepping technique based on a maximal Courant number has been adopted. The pressure velocity coupling is implemented through PISO (Pressure Implicit with Splitting of Operator) algorithm [7]. The absolute error tolerance criteria for pressure and velocity are set to 10^{-6}. The structural part has been solved by a large strain elastic stress analysis solver based on Lagrangian displacement formulation [8]. The absolute tolerance criterion of the structural solver is also taken to be 10^{-6}. A quasi-Newton coupling algorithm with an approximation for the inverse of the residual's Jacobian matrix from a least-square model (IQN-ILS) [6] has been adopted in the strong coupling method.

Computational Domain and Mesh

A two-dimensional rectangular computational domain of size 37.5Dx30D, as shown in Fig. 1(a), has been considered through a domain convergence study. The dimensions of the domain are shown in terms of the diameter of the cylinder D. Simulations are performed for varying gap (G), length (L) and thickness (T) of the structure. The results of the domain convergence study with three different domain sizes of 35Dx25D, 37.5Dx30D, 40Dx35D are shown in Fig. 2(a).

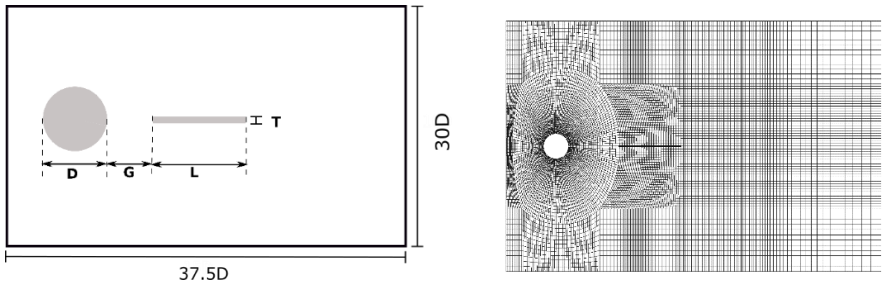

(a) Domain (b) Structured mesh

Figure 1: Computational domain (not to scale) and mesh.

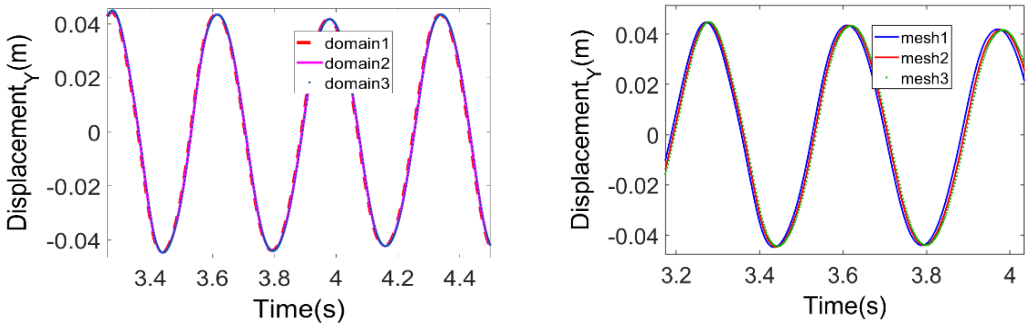

(a) Domain convergence (b) Mesh convergence

Figure 2: Domain and mesh convergence

Standard boundary conditions have been applied: a zero pressure gradient and a constant free-stream at the inlet; a zero velocity gradient and atmospheric pressure condition at the outlet; no slip and zero normal pressure gradient condition on the horizontal walls and traction boundary condition on the flexible flapper. The computational domain is discretized using structured grids as shown in Fig. 1(b). A mesh, containing 158 x 10^3 grid points, has been finalized through a grid independence test by comparing the results of three different mesh sizes, having 141 x 10^3, 158 x 10^3 and 181 x 10^3 grid points (Mesh 1, Mesh 2 and Mesh 3, respectively) at Re = 500; see Fig. 2(b).

Validation of the FSI Solver

The present FSI solver has been quantitatively validated with the benchmark case of a flexible splitter plate attached with a rigid cylinder, presented in the 'FSI2' case by Turek and Hron [9]. The mesh, chosen after grid independence study at Re = 500, has been used for the validation case at a lower Re = 100. The vertical tip displacement time-histories, representing a self-sustained periodic oscillatory state of the flexible plate, obtained from the present FSI simulations show excellent match with the results presented in [9].

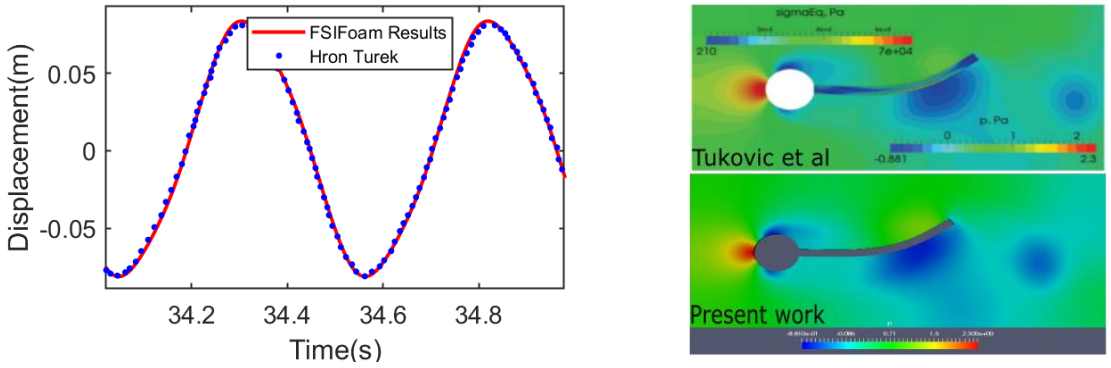

(a) Quantitative validation

(b) Qualitative validation

Figure 3: Computational domain (not to scale) and mesh.

Results

The parameters considered in this study are as follow: structure to fluid density ratio $\mu = \frac{\rho_s}{\rho_f}$=1; non-dimensional Young's modulus $\bar{E} = E/(\rho_f * u_m^2)$ = 5600; non-dimensional length L/D = 3; Reynolds number Re =500; the non-dimensional thickness of the filament T/D = 0.10. E is the dimensional Young's modulus of the structure; $u_m$is the mean uniformvelocity at the inlet. Non-dimensional gap between the cylinder and the filament G/D and transverse of the flexible flapper is varied in different cases. Two representative cases for upstream circular and elliptical

bluff bodies are presented here considering G/D = 2. The circular cylinder-flapper system is observed to generate a 2P vortex-street in the wake, as shown in Fig. 4(a). The body-bound vortices in the intermediate region of the bluff body and the flapper mildly deforms the extended shear layers of the bluff body, which contributes to a weak presence of quasi-periodicity in the response; the conclusive dynamical proofs for the existence of quasi-periodicity is beyond the scope of this document and will be shown in the presentation. The corresponding displacement envelope of the flexible flapper is presented in Fig. 4(b) and shows an organized pattern.

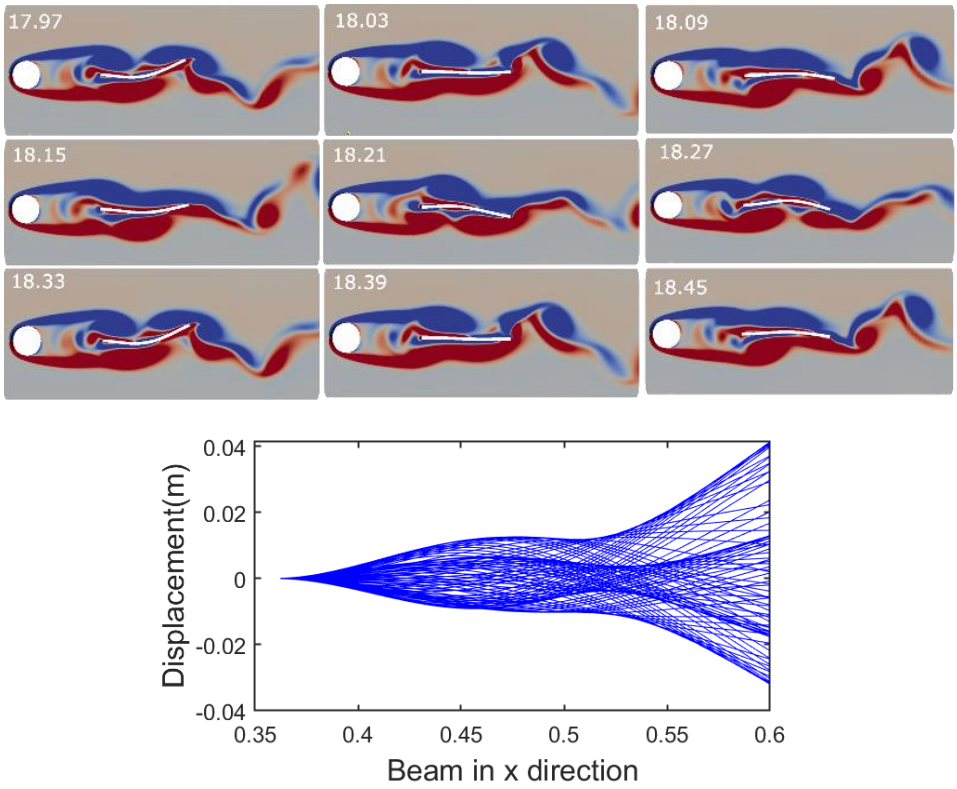

Figure 4: (a) Near Field Wake and (b) the displacement envelope of the flapper for the circular cylinder case.

On the other hand, in case of an elliptical bluff body, the rebound vortices are more powerful in the gap region. As a result, the shear layers are seen to be deformed significantly, thus triggering aperiodicity in the flapper response through stronger interactions. This can be seen from the near-field wake and the corresponding displacement envelop of the flapper, presented in 5(a) and 5(b), respectively. A detailed investigation has been carried out using robust time-series analysis tools to show the presence of aperiodicity in this case and will be demonstrated in the presentation.

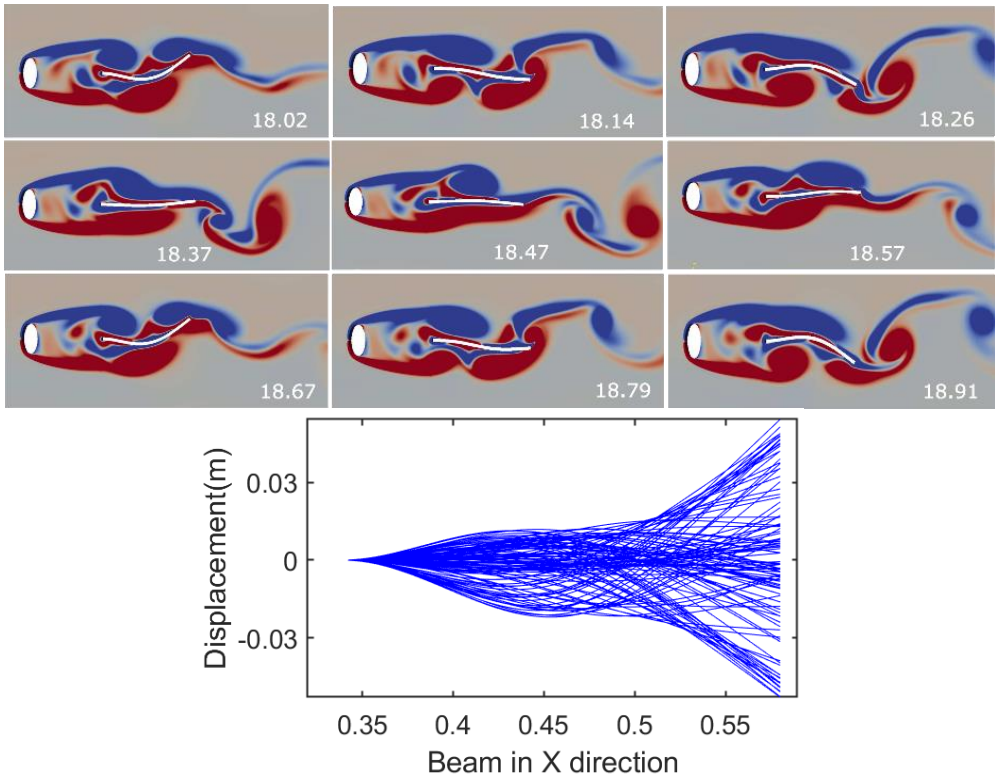

Figure 5: (a) Near-field wake and (b) the displacement envelope of the flapper for the elliptical cylinder case.

The present investigation of this FSI model with fsiFOAM solver reveals distinctly different dynamical regimes of periodicity and aperiodicity for different bluff-body shapes and different relative positions of the flexible flapper. The implications of these different dynamics on the energy harvesting potential are presently being investigated by the authors and will be presented in the conference. Since the solver achieved a better accuracy over the mesh discretisation [6], the more accurate results give more accurate dynamics in this kind of high-end computing. Though all simulations here are run in serial, the solver is designed for parallel processing and faster simulations, which are yet to be evaluated in our work.

References:

[1] S. Ramananarivo, R. Godoy-Diana, B. Thiria, Passive elastic mechanism to mimic fish-muscle action in anguilliform swimming, Journal of The Royal Society Interface 10 (88) (2013) 20130667.

[2] Y. Yu, Y. Liu, Flapping dynamics of a piezoelectric membrane behind a circular cylinder, Journal of Fluids and Structures 55 (2015) 347-363.

[3] R. Gopalkrishnan, M. S. Triantafyllou, G. S. Triantafyllou, D. Barrett, Active vorticity control in a shear flow using a flapping foil, Journal of Fluid Mechanics 274 (1994) 1-21.

[4] Y. Lau, R. So, R. Leung, Flow-induced vibration of elastic slender structures in a cylinder wake, Journal of Fluids and Structures 19 (8) (2004) 1061-1083.

[5] J. Degroote, R. Haelterman, S. Annerel, P. Bruggeman, J. Vierendeels, Performance of partitioned procedures in fluid-structure interaction, Computers & Structures 88 (7-8) (2010) 446{457.

[6] Ž Tuković,,A. Karać, P. Cardif, H. Jasak, A. Ivanković, OpenFOAM finite volume solver for fluid-solid interaction, Transactions of FAMENA 42 (3) (2018) 1-31.

[7] J. H. Ferziger, M. Perić, Computational methods for fluid dynamics, vol. 3, Springer, 2002.

[8] P. Cardif, Ž Tuković, H. Jasak, A. Ivanković, A block-coupled finite volume methodology for linear elasticity and unstructured meshes, Computers & Structures 175 (2016) 100-122.

[9] S. Turek, J. Hron, Proposal for numerical benchmarking of fluid-structure interaction between an elastic object and laminar incompressible flow, in Fluid-Structure Interaction, Springer, 371-385, 2006.